Physicochemical features of the formation of siliceous porous mesophases
1. General views on the mechanism

V. N. Romannikov, V. B. Fenelonov, A. V. Nosov, A. Yu. Derevyankin, S. V. Tsybulya, and G. N. Kryukova*

G. K. Boreskov Institute of Catalysis, Siberian Branch of the Russian Academy of Sciences, 5 prosp. Akad. Lavrent'eva, 630090 Novosibirsk, Russian Federation. Fax: +7 (383 2) 34 3056. E-mail: zeolite@catalysis.nsk.su

The formation of mesoporous mesophase materials *via* precipitation of soluble SiO_2 forms on the surface of cationic cetyltrimethylammonium micelles was studied. The main physicochemical factors determining the formation of siliceous mesoporous materials and providing an explanation of the observed changes in the structural and textural characteristics of the materials were identified and discussed.

Key words: mesophase mesoporous materials, structural and textural parameters, MAS ^{29}Si NMR.

After the publication of works of the Mobil company in the 90s,[1,2] a fundamentally new line in nanotechnology of inorganic material started to form. It is based on coprecipitation of an inorganic material with a surfactant (S), which is accompanied by self-assembly of liquid-crystal mesophases. Removal of the surfactant from the system yields a porous material, whose texture corresponds to a regular (*e.g.*, hexagonal) packing of cylindrical pores of a calibrated nanometer size with the appropriate long-range order and without a short-range order.[3—6] These mesoporous mesophase materials (MMM) have already become of substantial interest as acid—base and redox catalysts.[3,6,7]

Several possible mechanisms for the formation of MMM by the reactions of monomeric inorganic complexes (I) with surfactant molecules (S) are considered in the literature[2—5,8—24]; they include approaches based on nonspecific van der Waals interaction of neutral S^0I^0 molecules and those assuming an intermediate stage of formation of a covalent bond between these molecules, $S^0—I^0$.[5,8—13]

In systems involving ionic surfactants and ionic forms of the inorganic material, the most efficient interaction is due to the Coulomb forces between the oppositely charged S and I ions. Therefore, development of views on S^+I^- and S^-I^+ type mechanisms (*i.e.*, the simplest cases of ionic mechanisms) is now the most topical task. It is according to the S^+I^- reaction route that the most widely studied siliceous MMM are formed.[1,2,14—24] As a result of these studies, certain views on the mechanism of formation of these materials have taken shape; these views, providing a rough description of this mechanism, are outlined in several reviews.[3,5,6]

The first stage of this mechanism is interaction of silicate anionic species with the positively charged micelle surface of a cationic surfactant in an aqueous solution. The second stage, which also occurs at ~20 °C, involves self-organization of silylated micelles to give a primary organized mesophase. During the third stage, which is commonly carried out at elevated temperatures (≥70 °C) for relatively long periods, not only self-organization of the mesophase is completed but also polycondensation of the silicate anions occurs, which ensures the thermal stability of the inorganic framework.

However, this level of understanding is insufficient for optimization of the conditions of the synthesis of MMM that are important regarding the problems of catalysis. In this work, we start a systematic research into the mechanism of formation of these systems according to the ionic reaction route based on joint analysis of X-ray diffraction, structural, adsorption, textural, and spectral characteristics of MMM with a hexagonal type of packing. As the model system, we chose the MMM with the simplest chemical composition based on silica.

Experimental

Preparation of the initial forms of samples. SiO_2-MMM were synthesized using the methods described previously,[1,2,14,15,25,26] which involved hydrothermal treatment (HTT) of reaction mixtures with the molar ratio of components $SiO_2 \cdot 0.3C_{16}H_{33}NMe_3Br \cdot 0.3NaOH \cdot 102H_2O$ under static conditions at 120±5 °C over various periods of time (t) ranging from 0 to 404 h with subsequent filtration, washing, and drying at 30—40 °C. The time equal to 0 h corresponds to the material immediately after preparation of the mixture and its homogenization at room temperature. Sodium silicate was used as the source of SiO_2. The required concentration of NaOH was attained by neutralization using the calculated amount of sulfuric acid. The pH value of the initial and the final mixtures (*i.e.*, after the HTT) was the same (within the 10.5—11.5 range).

Thermal treatment of the initial forms of the samples was carried out in an air flow at 550—580 °C after they had been

Translated from *Izvestiya Akademii Nauk. Seriya Khimicheskaya*, No. 10, pp. 1845—1851, October, 1999.

1066-5285/99/4810-1821 $22.00

additionally dried at 120 °C. Since dry samples consisted only of $C_{16}H_{33}NMe_3^+$ cations and SiO_2 (the residual concentration of sodium did not exceed 0.05 % (w/w) Na_2O), the composition of the initial forms was calculated from the change in the weight upon annealing of the dry sample as $[C_{16}H_{33}N(CH_3)_3^+/SiO_2] = (NR_4^+/SiO_2)$.

The X-ray diffraction patterns were recorded for both the initial and calcined forms of air-dried samples on a URD-63 diffractometer using monochromatized Cu-Kα radiation (λ = 1.54178 Å) both for angles of 1° to 40° 2θ at a rate of 0.5 deg min^{-1} and by scanning of the angles of 1° to 7° 2θ with a step of 0.02° and an accumulation time at each point of 20 s. The latter recording conditions ensure an accuracy of calculation of a unit cell parameter of at least ±0.02 nm.

The electronic micrographs of calcined SiO_2-MMM were obtained on a JEM 2010 transmission microscope (resolution 0.14 nm, accelerating voltage 200 kV).

The true density of calcined SiO_2-MMM was measured against helium using an Autopycnometer-1320 instrument for freshly dried samples at 120 °C for 1.5—2 h. For the series studied, the density was 2.13±0.05 g cm^{-3}.

MAS ^{29}Si NMR spectra were recorded on a Bruker MSL-400 NMR spectrometer (79.49 MHz) at room temperature. The pulse duration was 3 μs (π/4), the delay between the pulses was 30 s, and the scan number was 1000—4000. The frequency of rotation of samples at a "magic" angle was 3.7 kHz. The chemical shifts were referred to external tetramethylsilane.

The adsorption characteristics were measured for calcined forms of samples using a Micromeritics ASAP-2400 setup by the nitrogen adsorption at ≅77 K *via* the standard procedure after evacuation at 350 °C for 12—16 h to a residual pressure of $<10^{-3}$ Torr. The textural parameters of the mesophases were calculated from the resulting isotherms of nitrogen adsorption by the method described previously.[23,24,27]

Results and Discussion

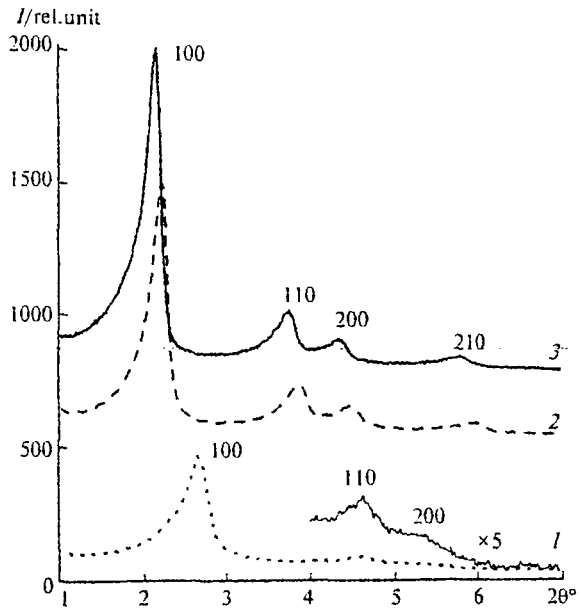

Fig. 1. X-ray diffraction patterns of the annealed forms of SiO_2-MMM: *1*, C16-0; *2*, C16-20; *3*, C16-404.

General X-ray diffraction patterns for both initial and annealed SiO_2-MMM forms (Fig. 1) are very close to those reported for similar systems (*e.g.*, in Ref. 25). When $t = 0$, the X-ray diffraction pattern of a sample includes three reflexes, and when $t \geq 3$ h, it includes four well-resolved reflexes in the region of very small angles (1—7° 2θ, see Fig. 1). No other reflexes can be observed up to an angle of 40° 2θ.

It can be seen from electron micrographs (Fig. 2) that the mesophase is formed as a close hexagonal packing of cylindrical pores. However, the degree of ordering is determined by the conditions of formation of SiO_2-MMM; indeed, on passing from sample C16-0 to C16-3 (*i.e.*, upon an increase in both the phase formation temperature from 20 to 120 °C and in the duration of the HTT from 0 to 3 h, see Fig. 2, *a*, *b*), the degree of

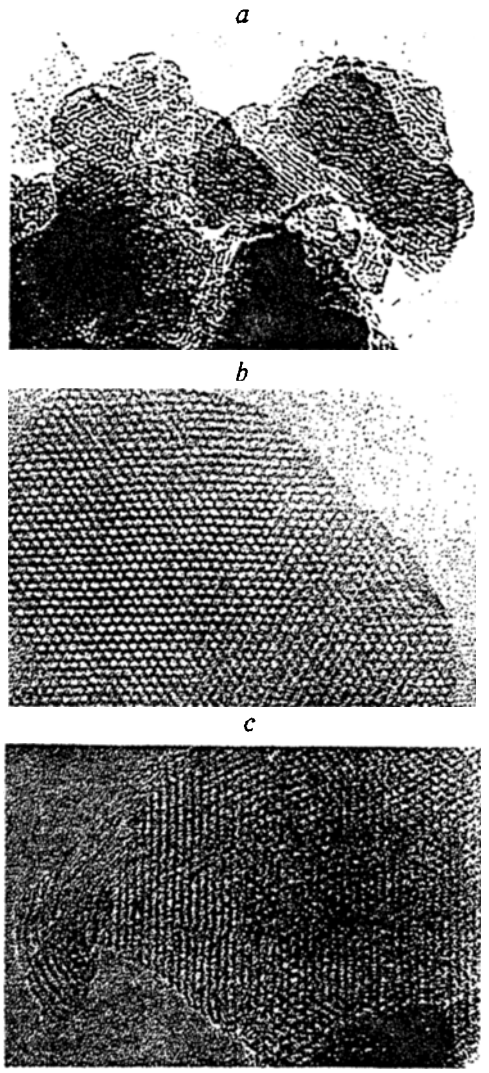

Fig. 2. Electron micrographs of the annealed forms of SiO_2-MMM: *a*, C16-0 (×500000); *b*, C16-3 (×900000); *c*, C16-404 (×700000).

ordering in the system substantially increases. In the approximation of perfect hexagonal packing, the reflexes observed on the X-ray diffraction patterns (see Fig. 1) are indicated as (100), (110), (200), and (210).

Table 1 presents the results of calculations of structural characteristics of all the systems studied both in the initial and annealed states. It can be seen that passing from C16-0 to C16-3 leads to a considerable increase in the unit cell parameter a_0 for both initial and annealed samples. On subsequent treatment ($t \geq 3$ h), the a_0 parameter no longer changes in either initial or the corresponding annealed forms. In addition, it can be seen from Table 1 that the (100) reflex appreciably narrows down as time increases (especially in the initial period, $t \leq 20$ h).

The above-described changes in the X-ray diffraction characteristics (see Table 1) are accompanied by a monotonic decrease in the mole fraction of the NR_4^+ surfactant cations in the initial forms of the SiO_2-MMM samples; the decrease in the (NR_4^+/SiO_2) ratio is especially pronounced on going from sample C16-0 to sample C16-3.

The typical patterns of the isotherms of nitrogen adsorption for the annealed forms of SiO_2-MMM and their comparative plots are shown in Fig. 3, *a* and 3, *b*, respectively. It can be seen from Table 2 that the numerical values for most of the textural parameters remain virtually constant. Attention is attracted only by the discontinous increase in the mesopore diameter on passing from C16-0 to C16-3. It can also be noted that the mesopore volume tends to increase somewhat as the duration of the HTT increases.

The MAS ^{29}Si NMR spectra for some of the SiO_2-MMM samples in the initial and annealed forms are presented in Fig. 4. The spectra of the initial forms (Fig. 4, *spectra 1—3*) exhibit two partially overlapping lines with δ −99 and −108, corresponding to silicon

Table 1. X-ray diffraction and chemical characteristics of SiO_2-MMM samples

Sample	Synthesis temperature/°C	Initial form			Annealed form		
		d_{100}	a_0	NR_4^+/SiO_2	d_{100}	a_0	$B(100)$
		nm		/mol	nm		/°2θ
C16-0	20	3.85	4.44	0.25	3.24	3.74	0.41
C16-3	120	4.19	4.84	0.21	3.95	4.56	0.23
C16-7	120	4.19	4.84	0.20	3.95	4.56	0.26
C16-20	120	4.19	4.84	0.20	3.95	4.56	0.24
C16-63	120	4.19	4.84	0.20	3.95	4.56	0.22
C16-188	120	4.22	4.87	0.20	3.95	4.56	0.22
C16-404	120	4.22	4.87	0.19	3.99	4.62	0.22

Table 2. Textural parameters of SiO_2-MMM samples in the annealed form

Sample	Specific surface area ($m^2\ g^{-1}$) of mesopores (A_{me})	Specific surface area ($m^2\ g^{-1}$) external (A_{ext})	V_{me} /$cm^3\ g^{-1}$	d_ε nm	h_w nm
C16-0	1173	82	0.810	3.12	0.62
C16-3	993	90	0.824	3.81	0.74
C16-7	984	99	0.850	3.84	0.72
C16-20	1083	84	0.885	3.87	0.69
C16-63	1107	64	0.942	3.90	0.65
C16-188	1105	36	0.939	3.90	0.65
C16-404	1114	57	0.951	3.96	0.65

Note. V_{me} is the mesopore volume, d_ε is the mesopore diameter, and h_w is the average wall thickness.

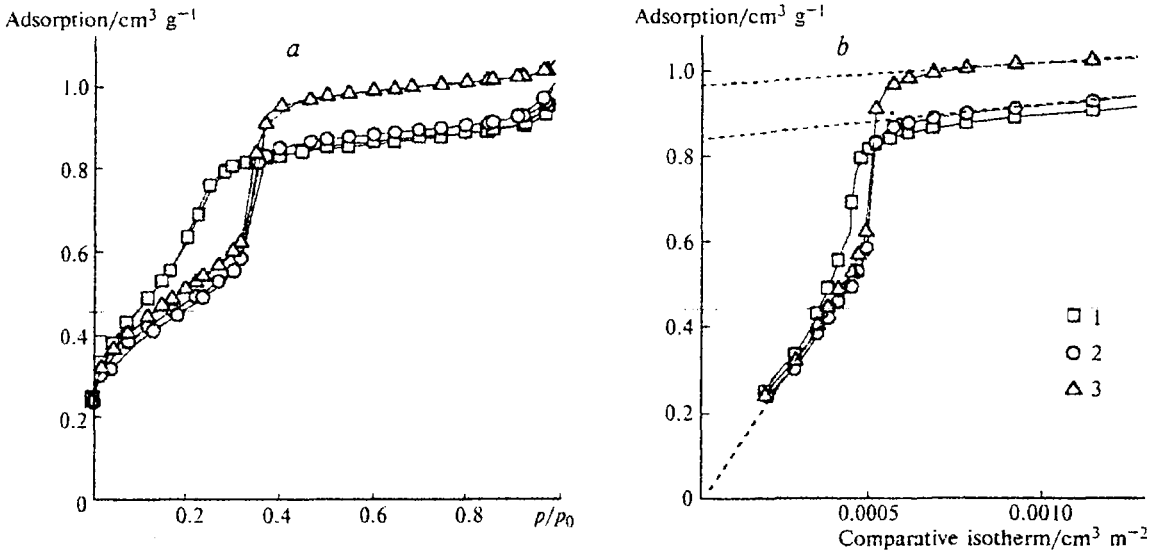

Fig. 3. Nitrogen adsorption isotherms (*a*) and their comparative plots (*b*) for the annealed forms of SiO_2-MMM: *1*, C16-0; *2*, C16-3; *3*, C16-404.

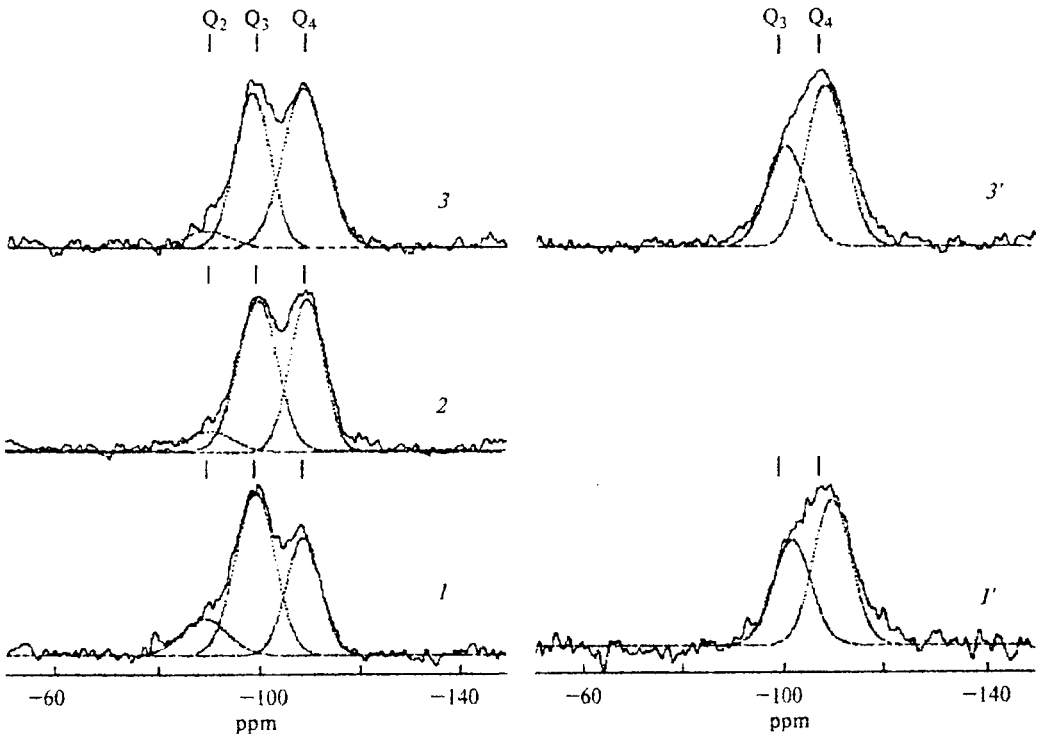

Fig. 4. MAS ^{29}Si NMR spectra of SiO_2-MMM samples in the initial (*1*, *2*, *3*) and annealed (*1'*, *3'*) forms. The resolution of the spectra into components is also shown: C16-0 (*1*, *1'*); C16-3 (*2*); C16-404 (*3*, *3'*).

atoms bound through oxygen bridges to three (Q_3) and four (Q_4) silicon atoms, respectively.[18] The spectra also contain a line at about δ −90, which is manifested as a shoulder of the signal at δ −99 and corresponds to silicon atoms in Q_2 coordination. After annealing of the SiO_2-MMM samples, the signal at δ −90 in the MAS ^{29}Si NMR spectra disappears and the relative intensity of the signal with δ −99 decreases (see Fig. 4, *1'*—*3'*).

Table 3 presents the results of quantitative estimates of the distribution of silicon atoms over the deconvolution states. The data were obtained by integration of the MAS ^{29}Si NMR spectra (see Fig. 4) after their resolution into the corresponding Gaussian components. It can be seen that an increase in both the synthesis temperature (samples C16-0, C16-3) and HTT duration (samples C16-3, C16-404) results in increased proportions of the Q_4 state of silicon atoms accompanied by decreased proportions of Q_3 and Q_2 states in the initial forms of the samples. Annealing of the initial forms always results in higher proportions of the Q_4 type state and largely levels out the difference in the distribution of silicon atoms over the states.

Table 3. Normalized distribution of silicon atoms over states in the SiO_2-MMM samples as a function of the composition (%) of the second coordination sphere based on the ^{29}Si NMR data

Sample	Initial form				Annealed form		
	Q_2	Q_3	Q_4	(Q_4/Q_3)	Q_3	Q_4	(Q_4/Q_3)
C16-0	14	53	33	0.62	46	54	1.17
C16-3	8	49	43	0.88	—	—	—
C16-404	6	42	52	1.24	41	59	1.44

The primary product and its properties

Some data published previously[18,25] and our experimental results indicate that the formation of SiO_2-MMM from soluble silicates and cetyltrimethylammonium salts by the S^+I^- reaction route occurs prior to the HTT when aqueous solutions of the required compounds are merely mixed at room temperature. Contrary to the recently reported data,[3] systems of the C16-0 type are thermally stable. Indeed, after the oxidative heat treatment at 550—580 °C, which removes surfactant cations, they retain not only a substantial volume of mesopores (see Table 2) but also an X-ray diffraction pattern including the (100) reflex and higher-order reflexes (see Fig. 1, curve *1*). This fact indicates that even at the stage of synthesis at $t = 0$, the system should be regarded as a primary mesophase with a hexagonal packing of cylindrical mesopores of diameter $d \approx 3.12$ nm and with average unit cell parameter $a_0 \approx 3.7$ nm (see Table 2).

Special measurements using the low-angle X-ray scattering method showed that at 20 °C, a model aqueous

solution of the surfactant with a $[H_2O/C_{16}H_{33}NMe_3Br] \cong 340$ molar ratio contains only single cylindrical micelles with an average diameter of ~3.6 nm and virtually no larger aggregates or structures. This provides grounds for assuming that it is these micelles that react with silicate anions according to the S^+I^- route upon mixing of the corresponding solutions. Meanwhile (see Table 1, sample C16-0), the primary mesophase contains ~4 moles of SiO_2 per mole of surfactant cations, *i.e.*, the proportion of ionized SiO_2 does not exceed 25%. Hence, most of the SiO_2 present in the mesophase can formally be regarded as being electrically neutral and not interacting electrostatically with the charged micellar surface. In this approximation, the composition of the primary mesophase can be represented as

$$\{(\alpha)[NR_4]^+[OSi(OH)_3]^-, \\ (1-\alpha)[Si(OH)_4]^0\},$$

where α is the (NR_4^+/SiO_2) molar ratio (see Table 1).

The electrically neutral component of the silicate mesophase is, apparently, nonordered (amorphous), which is confirmed by the absence of X-ray diffraction reflexes at $2\theta \geq 7°$. However, it can be seen from the micrograph (see Fig. 2, *a*) that this component, which serves as the basis for the subsequent formation of the wall in SiO_2-MMM, is distributed fairly uniformly over the intermicellar space of the primary product. Indeed, on the one hand, it is known[28] that if no electrically neutral component is present in the initial mixture, SiO_2-MMM is not formed at all. On the other hand, the thickness of the wall (h_w, Table 2) in all of the samples studied is approximately the same, 0.62—0.74 nm, which is close to the size of two silicon-oxygen tetrahedra. Meanwhile, in the case where the inorganic component is nonuniformly distributed in the intermicellar space, one should expect an inevitable decrease in the degree of ordering of the resulting mesophase material with sharply broadened X-ray diffraction reflexes, which must be due to increased scatter of the a_0 parameter. In addition, the micellar space itself in sample C16-0 (see Fig. 2, *a*) is not highly ordered; there are many local bends caused, in particular, by the fact that the surfactant micelles are apparently somewhat flexible and, hence, they are not perfect cylinders. This local disordering also leads to broadening of the (100) reflex (see Table 1, sample C16-0) and can also influence its observed integral intensity (the latter fact will be the subject of subsequent investigations).

Hydrothermal treatment and its consequences

The HTT of the primary mesophase in the mother liquor for ≥3 h at 120 °C changes substantially many characteristics of SiO_2-MMM.

First, the hexagonal unit cell parameter a_0 increases jumpwise (see Table 1, samples C16-0 and C16-3); subsequently, at $t \geq 3$ h, this parameter remains virtually constant. An abrupt change in the a_0 parameter after the HTT of the reaction mixture has also been observed previously[14] and has been interpreted as being due to a phase transformation of the layered primary phase into a mesophase with hexagonal packing. This interpretation does not seem correct. First, according to electron microscopy data (see Fig. 2, *a*), the primary mesophase of C16-0 consists of hexagonally packed elements. Second, the X-ray diffraction pattern of the primary mesophase both in the initial and annealed forms (see Fig. 1, curve *1*) exhibits three reflexes, which are well induced in the approximation of hexagonal packing and give the same value for the lattice parameter, namely, 4.44, 4.46, and 4.43 nm for the initial form and 3.75, 3.74, and 3.74 nm for the annealed form (the average a_0 values are given in Table 1).

The conditions for the synthesis of the C16-0 and C16-3 mesophases, which absolutely did not differ regarding the composition of the initial mixture and almost did not differ in duration, were, however, substantially different regarding the temperature, which was 20 and 120 °C, respectively. Apparently, it is this factor that is the main reason for the discontinuous increase in the unit cell parameter a_0, because the volume of the hydrocarbon part of the micelles increases on heating, *i.e.*, because they undergo thermal expansion. In fact, for the temperature range considered, the volume thermal expansion coefficients of liquid paraffins are $\sim 1.5 \cdot 10\ deg^{-1}$. This means that heating at 100 °C increases the volume by ~15%. The estimate of the actual volume expansion of the C16-0 and C16-3 mesophases gives a value of 18.5%. Thus, thermal expansion of micelles should increase the diameter of mesopores and this is observed in reality (see Table 2, samples C16-0 and C16-3).

Second, during the HTT, the proportion of silicon atoms coordinated in the Q_4 fashion in the initial SiO_2-MMM forms increases (see Table 3). This fact indicates that an increase in the HTT temperature and duration brings about an increase in the degree of polycondensation of the SiOH groups in neighboring silicon-and-oxygen tetrahedra. Indeed (see Table 3), in the annealed forms of samples, for which one should expect not only complete removal of the organic component but also the limiting dehydration of the silanol groups, the Q_4 type state predominates.

In general, the above-described processes result in virtually complete elimination of local disordering associated with micelle bending and improve considerably the long-range order of the mesophase structure (see Fig. 2, *b*, *c*). This is manifested in the X-ray diffraction pattern as a substantial narrowing of the (100) reflex (see Table 1), whose observed half-width can serve as the X-ray diffraction indicator for the degree of ordering of an MMM.

Third, the chemical composition of the initial SiO_2-MMM forms changes on heating (see Table 1), namely,

the concentration of alkyltrimethylammonium cations decreases; the most pronounced (almost discontinous) change in the composition occurs during the first several hours of the HTT. The above-mentioned changes in the surfactant concentration in the initial forms of C_{16}-SiO_2-MMM are apparently due to hydrolytic decomposition by the scheme

$$(C_{16}H_{33}NMe_3)^+(OH_2)^-(OSi(OH)_3) \longrightarrow (C_{16}H_{33}NMe_3)^+(OH)^- + (HOSi(OH)_3).$$

The rate and the degree of hydrolysis should increase with both an increase in the temperature and in the synthesis duration. Upon hydrolysis, the siliceous mesophase passes into a state in which the micellar surface and the silicate wall are no longer connected by electrostatic forces. The C_{16}-trimethylammonium cation is able to pass from the mesophase into the mother liquor; thus, the mesopores empty and the medium pH increases. Both factors should affect inevitably the state of the siliceous mesoporous material. It has been shown recently[22,23] that an increase in the HTT temperature to 150 °C or higher is accompanied by a further increase in the a_0 parameter in SiO_2-MMM (Table 4). However, unlike the relatively low-temperature syntheses, in this case, the mesophase exists over fairly short periods of time, equal to about 20 h at 150 °C.[23] Subsequently, the structure of SiO_2-MMM undergoes gradual irreversible degradation to give a dense (nonporous) SiO_2 phase with the specific surface area $A_{bet} \leq 170$ m^2 g^{-1} even after 96 h (see Table 4). When the temperature of the synthesis is 200 °C, the rate of the structure degradation is apparently so high that the formation of SiO_2-MMM cannot be detected.[17]

A rough view on the reaction route and the driving forces of the degradation of the SiO_2-MMM structure under hydrothermal conditions can be derived from analysis of the experimental results presented in various publications.

Table 4. Comparison of the structural and textural characteristics of annealed C_{16}-SiO_2-MMM samples prepared with various temperatures of hydrothermal treatment

Sample	T (°C) /t (h)[a]	a_0	d_{me}	V_{me}	h_w	A_{me}
		nm		/cm^3 g^{-1}	/nm	/m^2 g^{-1}
C16-0	20/1	3.74	3.12	0.81	0.62	1173
BTR[b]	70/72	4.30	3.44	0.63	0.86	810
C16-63	120/63	4.56	3.90	0.94	0.65	1107
TR3-20h[b]	150/20	4.68	3.90	0.78	0.78	970
Sample 1[c]	150/24	4.70	3.90	—	0.80	937
TR3-24h[b]	150/24	6.37	5.53	0.97	0.84	820
TR1-2d[b]	150/48	7.61	6.53	0.91	1.08	660
TR1-3d[b]	150/72	7.61	5.77	0.50	1.84	520
TR1-4d[b]	150/96	—	—	0.04	—	170

[a] Conditions of the synthesis.
[b] The designations of the samples and the data were taken from Ref. 23.
[c] The designation of the sample and the data were taken from Ref. 22.

It is known[29] that the chemical potential of a solid phase depends on its surface curvature and, in the first approximation, it can be written as follows:

$$\mu = \mu_\infty \pm (2\sigma V/r), \quad (1)$$

where μ and μ_∞ are the chemical potentials of a curved and a flat surface, respectively; σ and V are the surface tension and the molar volume of the condensed phase, respectively; $r/2$ is the average radius of the surface curvature ($2/r$ is the average surface curvature), "+" refers to a convex surface and "−" corresponds to a concave surface. A consequence of Eq. (1) is the dependence of the equilibrium solubility of a solid phase on the curvature of its surface, which is written as the Gibbs—Kelvin—Freindlich equation

$$C = C_\infty \exp(\pm 2sV/rRT) \approx C_\infty[1 \pm (2\sigma V/rRT)], \quad (2)$$

where C and C_∞ are the equilibrium solubility over curved and flat surfaces, respectively; R is the gas constant; and T is temperature. The external surface of the mesophase particles, at least the one parallel to the axis of the cylinders, is convex or nearly flat, whereas the internal surface of cylindrical mesopores of diameter d_ε has a negative curvature radius, $r = d_\varepsilon$. Thus, when mesopores get free of the surfactant molecules due to hydrolysis, a gradient of the chemical potential μ (Eq. (1)) and, hence, of the equilibrium concentrations C (Eq. (2)) should arise between the external surface of the particles and the internal surface of the mesopores; correspondingly, the siliceous material passes into the mesopore bulk until the mesopores are completely filled. When the degree of hydrolysis increases, other mesopores, whose diameter is larger than that of the partially built-over mesopores, would get free of the surfactant cations. In this case, the siliceous material would be transferred from the newly opened mesopores into the bulk of the partially built-over mesopores.

Generally, this mechanism also accounts for the formation of mesopores with an increased diameter and for the increase in the average thickness of the wall between them upon high-temperature HTT of siliceous mesophases in the mother liquor. More evidence for the validity of this scheme for building-over the mesopores having got free of the surfactant cations is provided by the fact that longer times of HTT under isothermal conditions (150 °C or higher) result in greater lattice parameters a_0 of the mesophase and, simultaneously, in its less perfect structure (the number of observed X-ray diffraction reflexes decreases and the reflexes are broadened[23]) (see Table 4). This implies that under the degradation conditions, the number of cylindrical mesopores in each particle of the mesophase monotonically decreases and the average distance between the generatrices of these cylinders (*i.e.*, the wall thickness) increases monotonically as the synthesis duration increases (see Table 4).

The results obtained indicate that the "liquid crystal templating" mechanism of the formation of SiO_2-MMM, considered most frequently in the literature, should be regarded as only the very first approximation. The real process of formation of mesoporous mesophase materials involves the influence of many important physicochemical factors such as homogeneity of the initial components, thermal expansion of the hydrocarbon part of the micelles, and hydrolysis of the ionized component of the mesophase at elevated temperatures. The half-width and, perhaps, the integral intensity of the reflexes should be regarded as the X-ray diffraction indications of the level of ordering of the MMM.

This work was financially supported by the Russian Foundation for Basic Research (Project No. 98-03-32390a).

References

1. C. T. Kresge, M. E. Leonowicz, W. J. Roth, J. C. Vartuli, and J. S. Beck, *Nature*, 1992, **359**, 710.
2. J. S. Beck, J. C. Vartuli, W. J. Roth, M. E. Leonowicz, C. T. Kresge, K. D. Schmitt, C. T.-Chu, D. H. Olson, E. W. Sheppard, S. B. McCullen, B. Higgens, and J. L. Schlenker, *J. Am. Chem. Soc.*, 1992, **114**, 10834.
3. A. Corma, *Chem. Rev.*, 1997, **97**(6), 2373.
4. A. Sayari and P. Liu, *Microporous Mesoporous Materials*, 1997, **12**, 149.
5. N. K. Raman, M. T. Anderson, and C. J. Brinker, *Chem. Mater.*, 1996, **8**, 1682.
6. A. Sayari, *Chem. Mater.*, 1996, **8**, 1840.
7. A. Corma, *Topics in Catalysis*, 1997, **4**, 249.
8. Y.-Y. Huang, T. J. McCarthy, and W. M. H. Sachtler, *Appl. Catal. A: General*, 1996, **148**, 135.
9. D. M. Antonelly and J. Y. Ying, *Angew. Chem. Int. Ed. Engl.*, 1995, **34**, 2014.
10. D. M. Antonelly and J. Y. Ying, *Chem. Mater.*, 1996, **8**, 874.
11. D. M. Antonelly and J. Y. Ying, *Angew. Chem. Int. Ed. Engl.*, 1996, **35**, 426.
12. D. M. Antonelly, A. Nakahira, and J. Y. Ying, *Inorg. Chem.*, 1996, **35**, 3126.
13. T. Sun and J. Y. Ying, *Nature*, 1997, **389**, 704.
14. A. Monnier, F. Schuth, Q. Huo, D. Kumar, D. Margolese, R. S. Maxwell, G. D. Stucky, M. Krishnamurty, P. Petroff, A. Firouzi, M. Janicke, and B. F. Chmelka, *Science*, 1993, **261**, 1299.
15. G. D. Stucky, A. Monnier, F. Schuth, Q. Huo, D. Margolese, D. Kumar, M. Krishnamurty, P. Petroff, A. Firouzi, M. Janicke, and B. F. Chmelka, *Mol. Cryst. Liq. Cryst.*, 1994, **240**, 187.
16. Q. Huo, D. I. Margolese, U. Ciesla, P. Feng, T. E. Gier, P. Sieger, R. Leon, P. M. Petroff, F. Schuth, and G. D. Stucky, *Nature*, 1994, **368**, 317.
17. J. S. Beck, J. C. Vartuli, G. J. Kennedy, C. T. Kresge, W. J. Roth, and S. E. Schramm, *Chem. Mater.*, 1994, **6**, 1816.
18. C.-F. Cheng, Z. Luan, and J. Klinowski, *Langmuir*, 1995, **11**, 2815.
19. A. Firouzi, D. Kumar, L. M. Bull, T. Besier, P. Sieger, Q. Huo, S. A. Walker, J. A. Zasadzinski, C. Glinka, J. Nicol, D. Margolese, G. D. Stucky, and B. F. Chmelka, *Science*, 1995, **267**, 1138.
20. D. Kushalani, A. Kuperman, G. A. Ozin, K. Tanaka, J. Garces, M. M. Olken, and N. Coombs, *Adv. Mater.*, 1995, **7**, 842.
21. S. Inagaki, Y. Sakamoto, Y. Fukushima, and O. Terasaki, *Chem. Mater.*, 1996, **8**, 2089.
22. A. Corma, Q. Kan, M. T. Navarro, J. Perez-Pariente, and F. Rey, *Chem. Mater.*, 1997, **9**, 2123.
23. A. Sayari, P. Liu, M. Kruk, and M. Jaroniec, *Chem. Mater.*, 1997, **9**, 2499.
24. M. Kruk, M. Jaroniec, R. Ryoo, and J. M. Kim, *Microporous Materials*, 1997, **12**, 93.
25. H.-P. Lin, S. Cheng, and C.-Y. Mou, *Microporous Materials*, 1997, **10**, 111.
26. A. C. Voegtlin, A. Matijasic, J. Patarin, C. Sauerland, Y. Grillet, and L. Huve, *Microporous Materials*, 1997, **10**, 137.
27. V. B. Fenelonov, V. N. Romannikov, and A. Yu. Derevyankin, *Microporous Mesoporous Materials*, 1999, **28**, 57.
28. J. Liu, A. Y. Kim, J. W. Virden, and B. C. Bunker, *Langmuir*, 1995, **11**, 689.
29. R. K. Iler, *The Chemistry of Silica*, J. Wiley, New York, 1979.

Received September 15, 1998;
in revised form December 12, 1998